

VERTICAL UNDULATOR EMITTANCE MEASUREMENT: A STATISTICAL APPROACH

K.P. Wootton*, R.P. Rassool, School of Physics, University of Melbourne, VIC, Australia
M.J. Boland, B.C.C. Cowie, R. Dowd, Australian Synchrotron, Clayton, VIC, Australia

Abstract

Direct measurement of low vertical emittance in storage rings is typically achieved via interferometric techniques. Proof of low vertical emittance is demonstrated by the measurement of a null radiation field, which is also the crux of the vertical undulator emittance measurement. Here we present strategies to improve the sensitivity to low vertical emittance beams. We move away from photon spectrum analysis to a statistical analysis of undulator radiation, showing the measured increase in signal-to-background. Reproducing simulations of previous work, we demonstrate that photon beam polarisation extends the linearity of the technique by several decades in emittance. These statistical and polarisation improvements to the signal-to-background allow realistic measurement of smallest vertical emittance.

INTRODUCTION

Measurements and simulations of vertical emittance using a vertical undulator are presented. In previous work, vertical undulators were observed as highly sensitive to the electron beam vertical emittance [1, 2]. In order to measure beams of smallest vertical emittance, a concerted effort has been made to understand and minimise systematic and statistical uncertainties.

ORBIT BUMPS

One of the most significant systematic uncertainties in this flux measurement is the size and transverse position of the pinhole mask. In particular, the technique is sensitive to vertical transverse offsets of the pinhole [1].

The technique employed previously aimed to simultaneously minimise the size and centring of the pinhole formed by closing four white beam blades. Instead in this work the blades are closed to the minimum possible aperture, and transverse orbit bumps are performed of the electron beam through the insertion device to optimise centring. The pinhole flux measured in vertical angular bumps through the insertion device is illustrated in Fig. 1, and for small amplitude bumps around the diffraction pattern central lobe in Fig. 2. The small angular bumps through the insertion device are used to recover the angular distribution of undulator radiation. As an approximation, the angular distribution of undulator radiation can be fitted by the double-slit

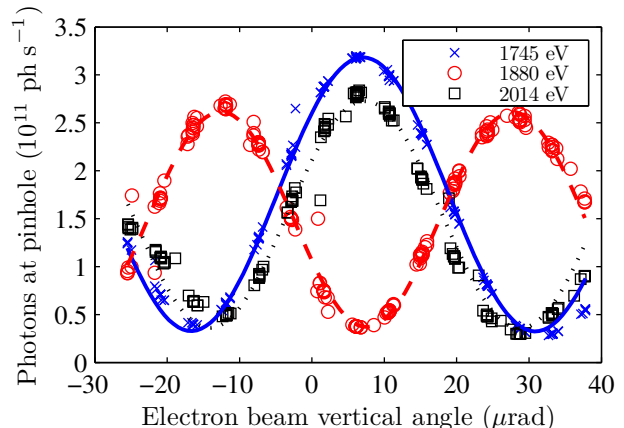


Figure 1: Insertion device photon flux measured and fitted for orbit bumps through the insertion device. Photon energies correspond to undulator harmonics 13, 14 and 15.

diffraction distribution [3]

$$I(\theta_y) = I(0) \text{sinc}^2 \left(\frac{2\pi\sigma_y\theta_y}{\lambda R_1} \right) \times \left[1 + \gamma \cos \left(\frac{2\pi\sigma_r\theta_y}{\lambda R_1} + \phi \right) \right], \quad (1)$$

where λ is the photon beam wavelength, R_1 the distance between the undulator and pinhole, σ_y is the electron beam vertical size, σ_r the transverse deflected amplitude of the electron beam in the undulator, γ the magnitude of the complex degree of spatial coherence, θ_y the angle of the orbit bump (or angle of observation of the photon beam) and ϕ an arbitrary phase offset (odd harmonic, $\phi \approx 0$, even harmonic, $\phi \approx \pi$). The transverse oscillation amplitude of the electron beam in the undulator is approximated by a double slit.

Fitting for the undulator radiation distribution, the angle of the electron beam through the insertion device can be varied to recover the angular distribution of undulator radiation, illustrated for small angles in Fig. 2.

REPEATED ACQUISITIONS

Statistical uncertainty in a measurement can be minimised by making repeated independent measurements of a single quantity [4]. We aim to measure the photon flux passing through a pinhole, for a given stored electron beam current. To compensate for the decaying electron beam current, the quantity measured here is photodiode drain cur-

* k.wootton@student.unimelb.edu.au

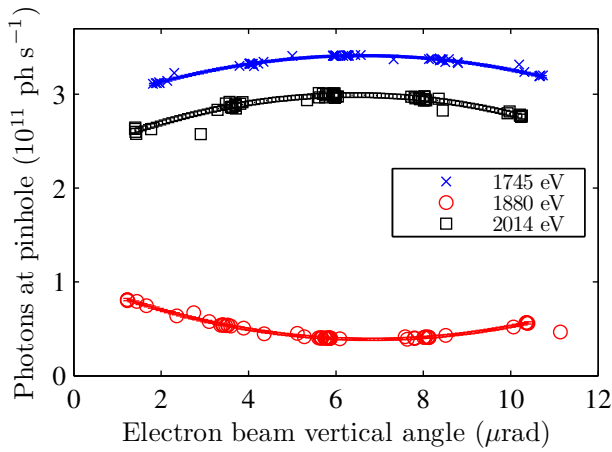


Figure 2: Measured and fitted vertical profile of undulator radiation through orbit bump. Photon energies correspond to undulator harmonics 13, 14 and 15.

rent, normalised to a nominal 200 mA stored beam current by the measured DCCT current. For n repeat measurements Gaussian-distributed about some mean value μ , the standard uncertainty in the estimate of the mean $\delta\mu$ is given by [4]

$$\delta\mu = \frac{\sigma}{\sqrt{n}}, \quad (2)$$

where σ is the standard deviation of measured values. The interpretation of this statement is that as the number of samples n is increased, the measured mean converges toward the true mean of the distribution. For comparison, in Figs. 3 and 4 the measured relative standard deviation is shown for 12 and 80 acquisitions, over various acquisition ranges and times. Figures 3 and 4 highlight that over appropriate

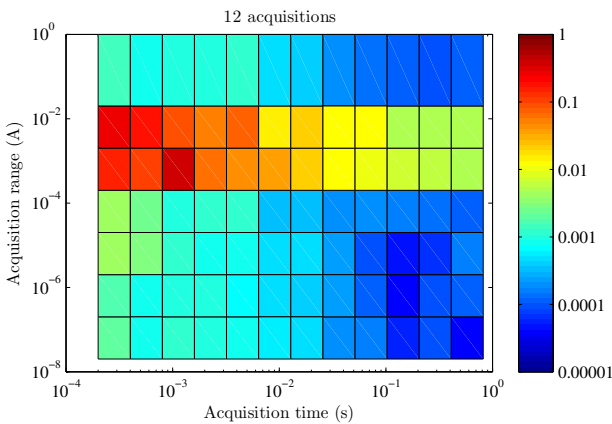


Figure 3: Relative standard uncertainty in diode current measured using a picoammeter over 12 acquisitions, for various acquisition times and current ranges. The mean diode current measured was approximately 1.1×10^{-7} A. The highest current range shown is the auto range. Colour scale shows measured $(\delta\mu/\mu)$.

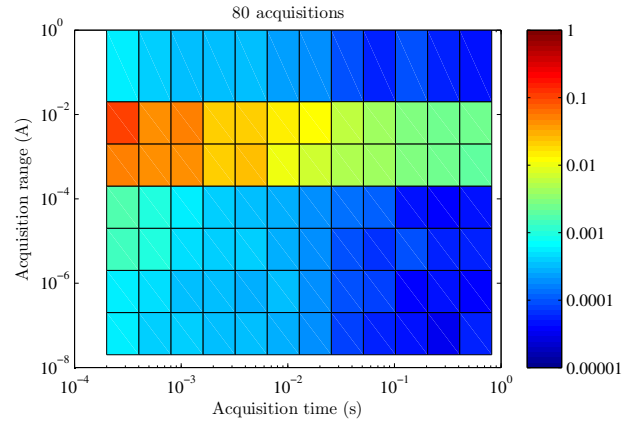


Figure 4: Relative standard uncertainty in diode current measured using a picoammeter over 80 acquisitions, for various acquisition times and current ranges. The mean diode current measured was approximately 1.1×10^{-7} A. The highest current range shown is the auto range. Colour scale shows measured $(\delta\mu/\mu)$.

choices of acquisition range, statistical uncertainty in the measured pinhole flux can be an insignificant contribution to the uncertainty in measured pinhole flux.

PHOTON POLARISATION

One approach in the minimisation of systematic uncertainties is by selective observation of the polarisation components of the photon beam flux. This was first outlined for a proposed SPring-8 vertical undulator measurement of vertical emittance [5]. The intensity of horizontal I_x and vertical I_y linear polarised light is described in terms of the Stokes parameters by [6]

$$I_x = 1 \times S_0 + 1 \times S_1 + 0 \times S_2 + 0 \times S_3, \quad (3)$$

$$I_y = 1 \times S_0 - 1 \times S_1 + 0 \times S_2 + 0 \times S_3, \quad (4)$$

where the Stokes parameters are defined in terms of the intensity of light with respect to polarisation orientations S_1 denotes linear polarisation, S_2 linear at 45° , and S_3 circular polarisation [7],

$$S_0 = 2I_0, \quad (5)$$

$$S_1 = 2I_1 - 2I_0, \quad (6)$$

$$S_2 = 2I_2 - 2I_0, \quad (7)$$

$$S_3 = 2I_3 - 2I_0. \quad (8)$$

We have undertaken simulations of the undulator brilliance using the SPECTRA code [8]. The code returns several polarisation parameters in the form,

$$I_0 = S_0, \quad (9)$$

$$PL = S_1/S_0, \quad (10)$$

$$PL45 = S_2/S_0, \quad (11)$$

$$PC = S_3/S_0. \quad (12)$$

Hence, we can calculate the intensities of horizontally and vertically polarised light as given by Eq. 3, 4 by

$$I_x = I_0(1 + S_1/S_0), \quad (13)$$

$$I_y = I_0(1 - S_1/S_0). \quad (14)$$

This simulation is presented in Fig. 5 for an ideal sinusoidal undulator and beam with parameters matching our experimental conditions [1]. It is seen that a significant contribution to the on-axis brilliance of even harmonics arises from horizontally polarised light. The ratio of fluxes for the 14th and 15th undulator harmonics with varying emittance is presented in Fig. 6. It can be seen that the measurement

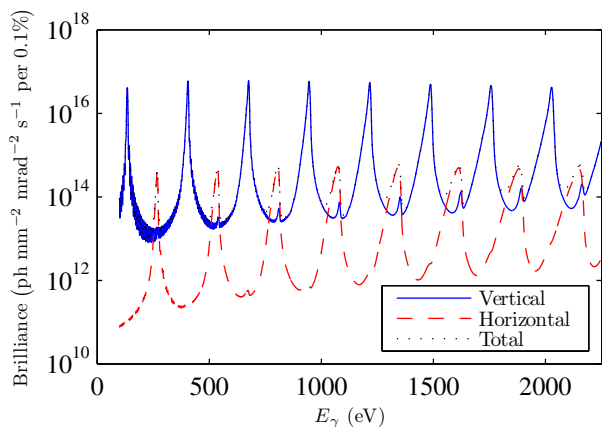


Figure 5: SPECTRA simulation [8] of spectral brilliance assuming an ideal undulator magnetic field, for horizontal and vertical photon polarisations. Vertical emittance $\varepsilon_y = 1$ pm rad.

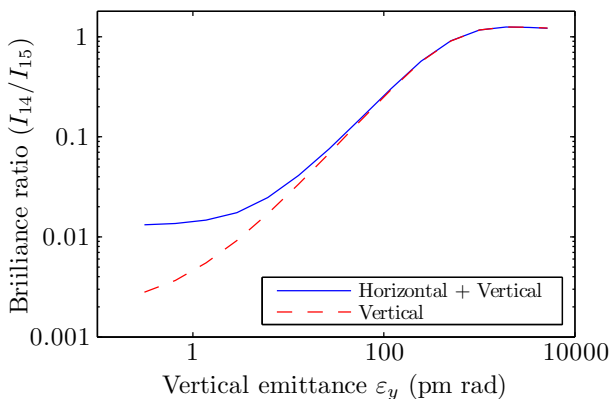


Figure 6: SPECTRA simulation [8] of the flux ratio of adjacent undulator harmonics, for total flux and vertical polarisation alone.

of the vertically polarised component of undulator radiation extends the linearity of the measurement technique to lowest vertical emittances. The next stage of investigation will be to repeat these brilliance calculations with measured magnetic fields of the insertion device, to account for phase errors of a real device.

CONCLUSION

The measurement of a null radiation field is the crux of this vertical emittance measurement. Techniques are presented to minimise sources of statistical and systematic uncertainty. To reconstruct the angular distribution of undulator radiation, transverse orbit bumps of the electron beam are promising, as is the rejection of horizontal polarised photons for the measurement of lowest vertical emittance.

ACKNOWLEDGEMENTS

KPW thanks S. Takano (Spring-8), C. Bloomer and E. Longhi (Diamond) for useful discussions at and following IBIC'12. This research was undertaken on the soft x-ray beamline on the storage ring at the Australian Synchrotron, Victoria, Australia.

REFERENCES

- [1] K.P. Wootton, et al. Phys. Rev. Lett. **109** (19), 194801 (2012).
- [2] K.P. Wootton, et al. Proceedings of IBIC 2012, Tsukuba, Japan, MOCB04 (2012).
- [3] M. Katoh and T. Mitsuhashi, Proceedings of PAC 1999, New York, USA, WEP22, March, (1999).
- [4] Evaluation of measurement data – Guide to the expression of uncertainty in measurement, Bureau International des Poids et Mesures, JCGM 100:2008, September (2008), <http://www.bipm.org/en/publications/guides/gum.html>.
- [5] S. Takano, ‘On emittance diagnostics of electron beam by observing synchrotron radiation from a vertical undulator’, Proceedings of Workshop on Precise Measurements of Electron Beam Emittances, KEK Proceedings 97-20, 18-19 October, 1997 (1998).
- [6] G. G. Stokes, Trans. Cambridge. Phil. Soc. **9** (3), 399–416 (1852).
- [7] E. Hecht, *Optics, 4ed.*, Pearson Education, San Francisco, CA, USA (2002).
- [8] T. Tanaka and H. Kitamura, J. Synch. Rad. **8**, 1221 (2001).